Supplementary Information

Conjugated Linker Unit Enables Self Assembly Monolayer Showing Higher Coverage of the Hole Transport Layer in Organic Solar Cells

Zekun Chen[1, 2], Xiaojun Li[1]*, Shucheng Qin[1], HaoZhe He[1, 2], Yuechen Li[1, 2], Meng Yuan[1, 2], Lei Meng[1, 2], Yongfang Li[1, 2, 3] *

[1] *Beijing National Laboratory for Molecular Sciences, CAS Key Laboratory of Organic Solids, Institute of Chemistry, Chinese Academy of Sciences, Beijing 100190, China.*
[2] *School of Chemical Science, University of Chinese Academy of Sciences, Beijing 100049, China.*
[3] *Laboratory of Advanced Optoelectronic Materials, College of Chemistry, Chemical Engineering and Materials Science, Soochow University, Suzhou 215123, China.*

*Corresponding authors (email: lixiaojun@iccas.ac.cn; liyf@iccas.ac.cn)

Supplementary Methods

Materials and synthesis: All chemicals and solvents were purchased from Innochem, J&K, Alfa Ae-sar and TCI Chemical Co. Commercial polymer donor PM6, small molecule acceptors (SMAs) BTP-eC9 were purchased from Organtec. The solvents do not need to degas in all the reactions, and the reactions all performed under nitrogen atmosphere. The synthetic route of MeOF-NaPACz are shown in Figure S1 where **1** was synthesized according to the procedures reported in the literature.[1] The detailed synthesis processes are described in the following.

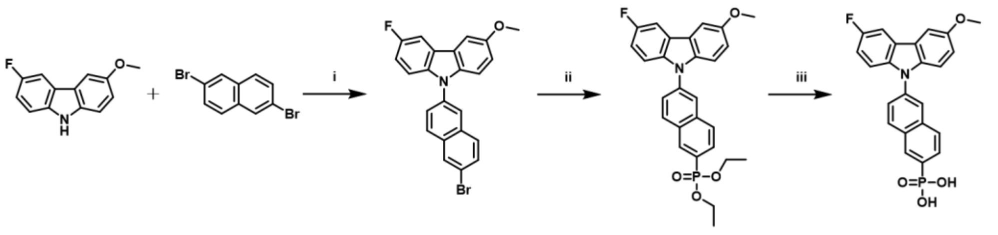

1 2 3 4

Figure S1. Synthesis routes of MeOF-NaPACz. Reagents and conditions: (i) 1,4-dibromobenzene, CuI, K_2CO_3, DMAc, 180 °C, 24h; (ii) diethyl phosphite, $Pd(OAc)_2$, dppf, KOAc, toluene, reflux, 24 h; (iii) Trimethylbromosilane, CH_2Cl_2, 25 °C, 12 h.

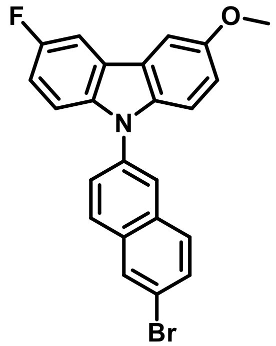

Synthesis of 9-(6-bromonaphthalen-2-yl)-3-fluoro-6-methoxy-9H-carbazole (2). **1**(800 mg, 3.72 mmol) and 2,6-dibromonaphthalene (4.21 g, 14.88 mmol) were dissolved in 25 mL N,N-Dimethylacetamide (DMAc), and K_2CO_3 (1.60 g, 11.60 mmol) and CuI (0.40 g, 2.12 mmol) were added subsequently. The mixture was stirred at 180 °C for 24 h. After cooling to room temperature, the resulting mixture was washed with water and extracted with dichloromethane. The combined organic layer was dried over anhydrous $MgSO_4$. After the solvent was evaporated under reduced pressure, the crude product was purified by column chromatography on silica gel (petroleum ether/dichloromethane = 4 :1 as the eluent) to give **2** as a colorless crystal (1.09 g, 70%). ^{1}H NMR (300 MHz, Chloroform-*d*) δ 8.15 (s, 1H), 7.99 (d, *J* = 7.8 Hz, 2H), 7.84 – 7.74 (m, 2H), 7.69 (t, *J* = 7.3 Hz, 2H), 7.58 (d, *J* = 2.5 Hz, 1H), 7.39 (dd, *J* = 9.0, 3.2 Hz, 2H), 7.22 – 7.06 (m, 2H), 3.98 (s, 3H).

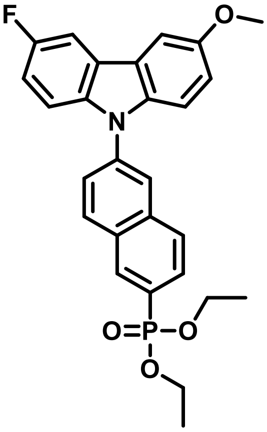

Synthesis of diethyl (6-(3-fluoro-6-methoxy-9H-carbazol-9-yl)naphthalen-2-yl)phosphonate (3). **2** (595 mg, 1.42 mmol), diethyl phosphite (0.3 mL, 2.13 mmol), $Pd(OAc)_2$ (16 mg 0.071 mmol), dppf (79 mg 0.142 mmol) and potassium acetate (420 mg 4.26 mmol) were dissolved in 25 mL of dry toluene under a nitrogen atmosphere. The mixture was heated to 110 °C for 24 h. After cooling to room temperature, the solvent was removed under the reduced pressure. The resulting mixture was washed with saturated brine and extracted with ethyl acetate. The organic layer was dried over anhydrous $MgSO_4$, and the solvent was removed under reduced pressure. The crude product was purified by column chromatography on silica gel (CH_2Cl_2: CH_3OH = 50:1) to give 3 as a colorless solid (542 mg, 80%). ^{1}H NMR (300 MHz, Chloroform-*d*) δ 8.48 (d, *J* = 15.4 Hz, 1H), 8.09 (d, *J* = 8.7 Hz, 1H), 7.98 (d, *J* = 2.0 Hz, 1H), 7.91 (dd, *J* = 8.5, 4.0 Hz, 1H), 7.79 (ddd, *J* = 10.0, 8.4, 1.4 Hz, 1H), 7.69 (dt, *J* = 8.7, 2.4 Hz, 2H), 7.49 (d, *J* = 2.5 Hz, 1H), 7.39 – 7.29 (m, 2H), 7.14 – 6.97 (m, 2H), 4.27 – 3.99 (m, 4H), 3.89 (s, 3H), 1.31 (t, *J* = 7.0 Hz, 6H).

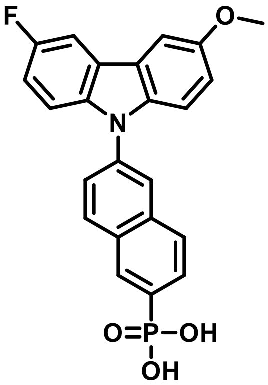

Synthesis of (6-(3-fluoro-6-methoxy-9H-carbazol-9-yl)naphthalen-2-yl) phosphonic acid(MeOF-NaPACz). **3** (307 mg, 0.729 mmol) was dissolved in 30 mL CH_2Cl_2. Trimethylbromosilane (0.6 mL, 5.30 mmol) was slowly added dropwise. The mixture was stirred at room temperature for 12 h. The resulting mixture was quenched with 10 mL of MeOH, followed by the addition of 20 mL of CH_2Cl_2, and stirred for 1 h. The solvent was evaporated under reduced pressure. After filtration, the solid was washed with water and diethyl ether to give MeOF-NaPACz as a white solid (249 mg, 80%). ^1H NMR (300 MHz, DMSO-d_6) δ 8.44 (d, J = 14.8 Hz, 1H), 8.34 (d, J = 8.8 Hz, 1H), 8.28 – 8.21 (m, 1H), 8.13 (ddd, J = 9.1, 6.5, 3.0 Hz, 2H), 7.90 (d, J = 2.5 Hz, 1H), 7.88 – 7.75 (m, 2H), 7.53 – 7.38 (m, 2H), 7.28 (td, J = 9.1, 2.7 Hz, 1H), 7.11 (dd, J = 9.0, 2.6 Hz, 1H), 3.89 (s, 3H), 3.17 (s, 2H). ^{13}C NMR (75 MHz, DMSO) δ 159.07, 154.64, 137.48, 136.41, 136.26, 135.08, 133.77, 131.66, 131.38, 131.16, 128.38, 128.19, 127.96, 125.74, 124.64, 124.14, 124.01, 123.62, 116.58, 114.54, 114.20, 111.38, 106.75, 104.27, 56.22, 49.07, 40.82, 40.54, 40.27, 39.99, 39.71, 39.43, 39.15. HRMS (MALDI-TOF), Calcd for $C_{23}H_{17}FNO_4P$ $[M+H]^+$: 421.0879; Found: 421.0876.

General characterization:

^1H NMR and ^{13}C NMR spectra were recorded using a Bruker AV-300 spectrometer in a *d*-chloroform solution at 300 K, unless specified otherwise.^{31}P NMR spectra were recorded using a Bruker AV-600 spectrometer in a *d*-DMSO solution at 300 K, Chemical shifts are reported as *δ* values (ppm) with tetramethylsilane (TMS) as a benchmark. High-resolution matrix-assisted laser desorption ionization time-of-flight mass spectrometry (MALDI-TOF) was performed on a Shimadzu spectrometer. UV-vis absorption spectra were recorded on the Hitachi U-3010 UV-vis spectrophotometer. For the film measurements, MeOF-4PACz and MeOF-NaPACz solutions in Isopropyl alcohol. The cyclic voltammetry (CV) measurement was performed on the Zahner IM6e electrochemical workstation, using a glassy carbon electrode as the working electrode, platinum wire as the counter electrode and Ag/AgCl as the reference electrode, at a potential scanning rate of 50 mV s^{-1} in 0.1 M tetrabutylammonium hexafluorophosphate (Bu_4NPF_6) acetonitrile solution. The ferrocene/ferrocene (Fc/Fc^+) pair was used as an internal reference. X-ray Photoelectron spectroscopy (XPS) data and Ultraviolet photoelectron spectroscopy (UPS) data were obtained through Kratos AXIS ULTRA DLD spectrometer. Non monochromatic He I (21.22 eV) source was used as an excitation source. Gold was used as reference. The bias voltage applied during the test is -9 V.

XPS semi-quantitative analysis

The difference coefficient is defined as follows:

$$\frac{R_{\mathrm{ASF}}}{R_{\mathrm{number}}}=\frac{\frac{I_{\mathrm{C}}/S_{\mathrm{C}}}{I_{\mathrm{P}}/S_{\mathrm{P}}}}{n_{\mathrm{C}}/n_{\mathrm{P}}}=\frac{R_{\mathrm{intensity}}}{R_{\mathrm{number}}}\times\frac{S_{\mathrm{P}}}{S_{\mathrm{C}}} \qquad \textbf{Equation S1}$$

Where R_{ASF}, R_{number} and $R_{\mathrm{intensity}}$ are the atomic-sensitivity-factors-weighted element ratio, stoichiometric ratio and XPS intensity ratio of C/P, respectively. I_{C} and I_{P} are element intensities, and n_{C} and n_{P} are the stoichiometric element number. S_{C} and S_{P} are atomic-sensitivity-factors, and they are 0.25 (C1s) and 0.39 (P 2p).

DFT calculation

All calculations are performed by ORCA (*version 5.0.4*). The geometries were optimized using function of ωB97X-D3 with def2-SVP basis set. Energy levels and molecular orbitals were calculated under B3PW91/def2-TZVP. ESPs and molecular dipole moments were performed under ωB97M-V/def2-SVPD. Wavefunction analysis were performed by Multiwfn (*version 3.8 dev branch-2023-Dec-1*) and VMD (*version 1.9.4*) was used for visualization.

The VASP code was employed to carry out all first-principles calculations. A revised Perdew-Burke-Ernzerhof generalized gradient approximation (PBEsol) was used for the exchange-correlation. Valence-core interactions were described by projector-augmented-wave (PAW) pseudopotentials. Plane-wave expansions with kinetic energies up to 600 eV was chosen as the basis set for all geometry optimization calculations. Surface atomic positions were allowed to relax, and others were fixed. 2 × 2 × 1 supercell was constructed and 1 × 1 × 1-center k-point mesh was adopted for calculation. The results were visualized by VESTA (*version 3.5.8*).

Fabrication and characterization of OSCs

The structure of all OSCs adopts the conventional device structure, ITO/HTL/active layer/PDINN/Ag structure. The SAM molecules were dissolved in absolute isopropyl alcohol with a concentration of 0.3 mg/ml and left to stir at room temperature for 1 hour. The SAM solution was placed into an ultrasonic bath for 15 min before use. The pre-patterned ITO glass substrate (sheet resistance = 15 Ω sq^{-1}) was sonicated sequentially in detergent, deionized water, acetone, and isopropanol, and then subjected to 40 minutes in an ultraviolet ozone chamber (Jelight Company, USA) UV treatment. The SAM molecules solution (50 µl for a 2.5×2.5 cm^2 substrate) was applied directly onto the ITO substrate for 10 s followed by a spin-coating step at 3000 rpm for 30 s. The ITO/SAM substrate was then placed onto a hotplate and annealed at 110 °C for 10 min. The PM6:SMA (D:A=1:1.2) was dissolved in oxylene (20 mg mL^{-1} in total). The blended solution was spin-coated on the ITO/HTL substrate at 3000 rpm for 30s. It is then annealed at 100°C for 10 minutes. Then PDINN methanol solution with a concentration of 1.0 mg mL^{-1} was deposited on the active layer at a speed of 3000 rpm for 30 seconds to provide a PDINN cathode modification layer. After cooling to room temperature, the sample was transferred to the evaporation chamber. Under the pressure of 1 × 10^{-5} Pa, about 100 nm of Ag electrode was evaporated and deposited. The device area is 6.0 mm^2. The current density-voltage (*J-V*) characteristics of OSCs were measured in a nitrogen glove box equipped with a Keithley 2450 Source Measure Unit in a glove box filled with nitrogen (oxygen and water contents are smaller than 0.1 ppm), using Oriel Sol3A Class AAA Solar Simulator (model, Newport 94023A) with 450W xenon lamp and air quality (AM) 1.5 filter as the light source. The light intensity was calibrated to 100 mW cm^{-2} by Newport Oriel 91150V reference cell. The external quantum efficiency (EQE) value was measured by the solar cell spectral response measurement system QER3-011 (Taiwan Enli Technology Co., Ltd.). The light intensity at each wavelength was calibrated with a standard single-crystal Si photovoltaic cell. In the Photo-CELIV and TPC measures, the OSCs were fabricated with the same method as mentioned above. The data were obtained by the all-in-one characterization platform, Paios (Fluxim AG, Switzerland). In the photo-CELIV measurement, the delay time is set to 0 s, the light intensity is 100%, the light-pulse length is 100 μs, finally the sweep ramp rate rises from 20 V ms^{-1} to 100 V ms^{-1}. In the TPC and TPV measurement, the light intensity is 10.0%, 17.8%, 31.6%, 56.2% and 100.0%, respectively, and settling time is 100 μs, pulse length is 100 μs and the follow-up time is 200 μs.

Conductive atomic force microscopy (c-AFM), Kelvin probe force microscopy (KPFM) and Atomic Force Microscope (AFM)

C-AFM, KPFM and AFM data were acquired *via* Bruker Dimension Kelvin probe force microscopy in Potential Channel equipped with PFQNE-AL probe, which is a platinum-iridium coated tip with a frequency of ≈300 kHz and a nominal tip radius of ≈5 nm. To calibrate the KPFM measurements, we developed a method using an Al Si-Au standard. The average contact potential distribution (CPD) profile was extracted from the calibration sample, and the work function of the tip (W_F^{tip}) was calculated using the value of the CPD in the gold region (W_F^{Au}) as $W_F^{tip} = W_F^{Au} - eCPD$. The measurements were performed on Bruker Dimension ICON, with the sample fixed in a custom-made vertical sample holder. The chamber was filled with high-purity nitrogen to minimize the influence of ambient conditions on the measurements.

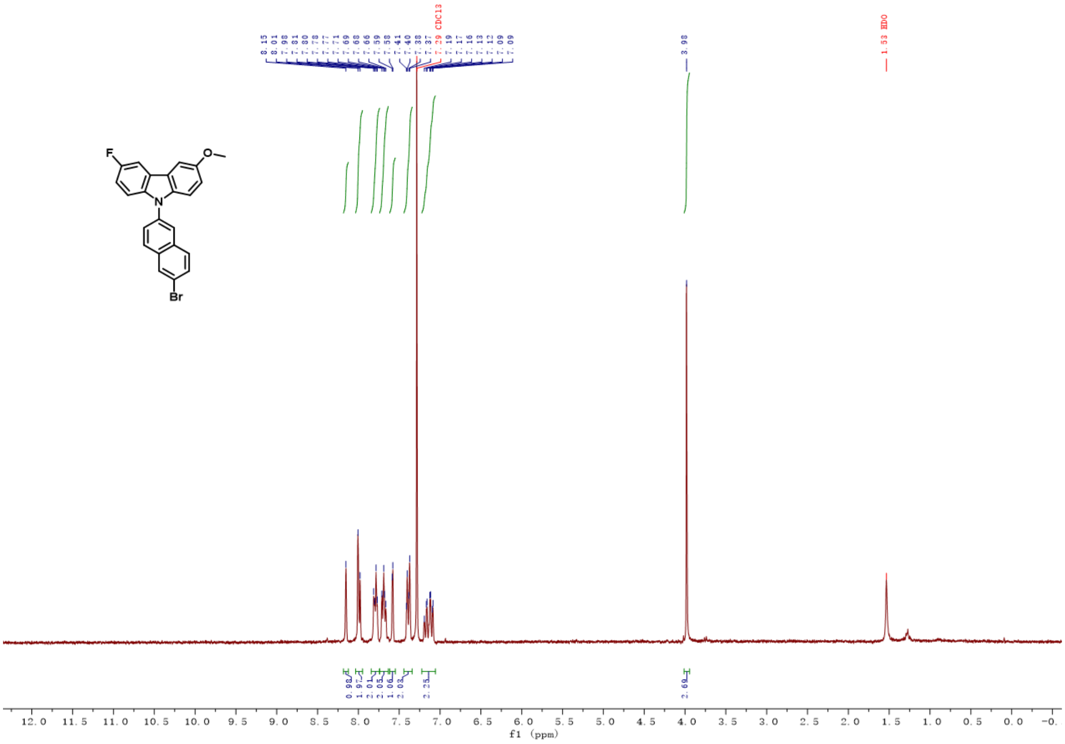

Figure S2. ^{1}H NMR spectrum of **2** in $CDCl_3$.

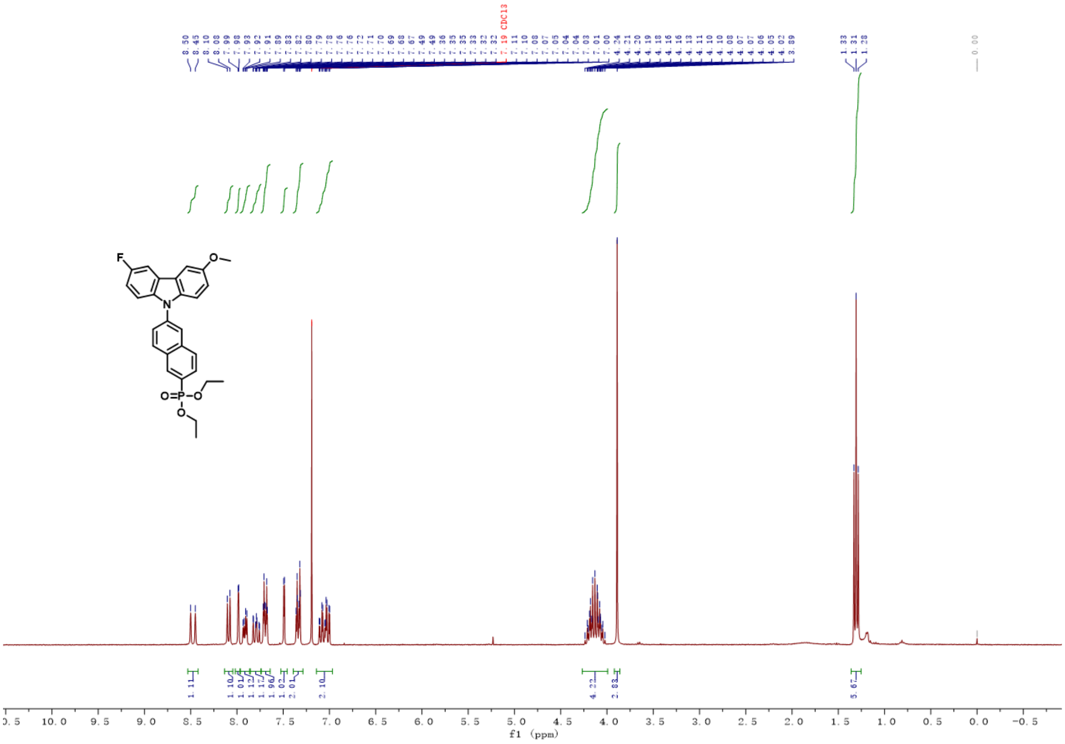

Figure S3. ^{1}H NMR spectrum of **3** in $CDCl_3$.

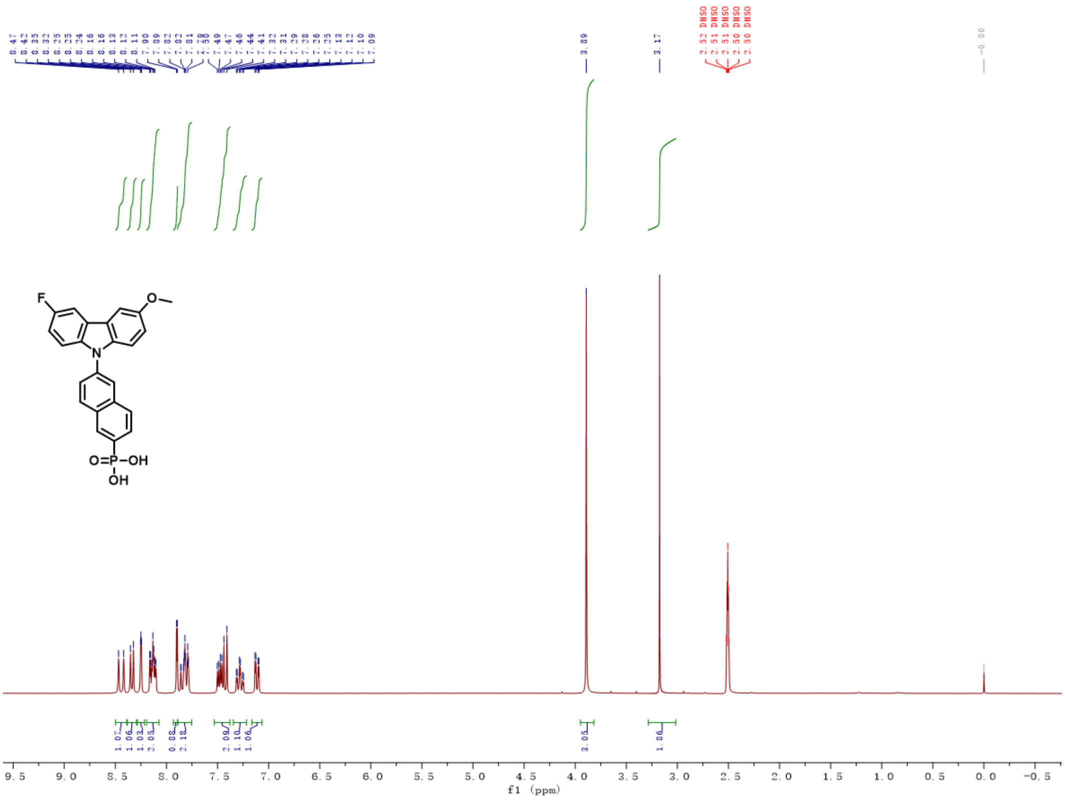

Figure S4. ^{1}H NMR spectrum of MeOF-NaPACz in DMSO-d_6.

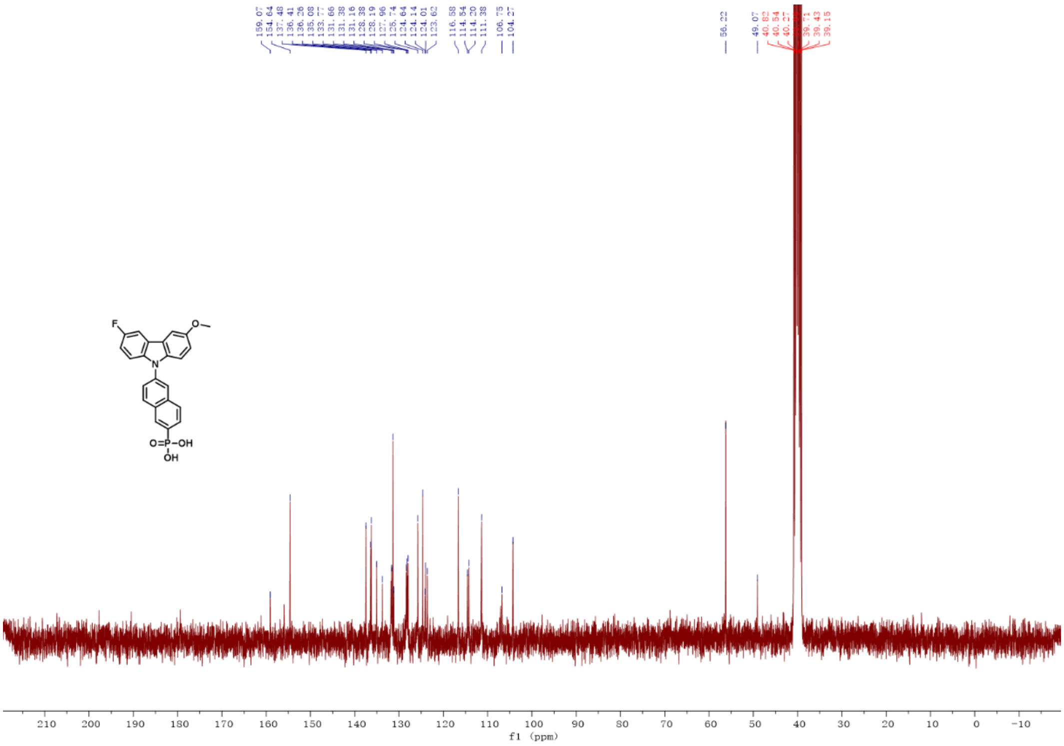

Figure S5. ^{1}C NMR spectrum of MeOF-NaPACz in DMSO-d_6.

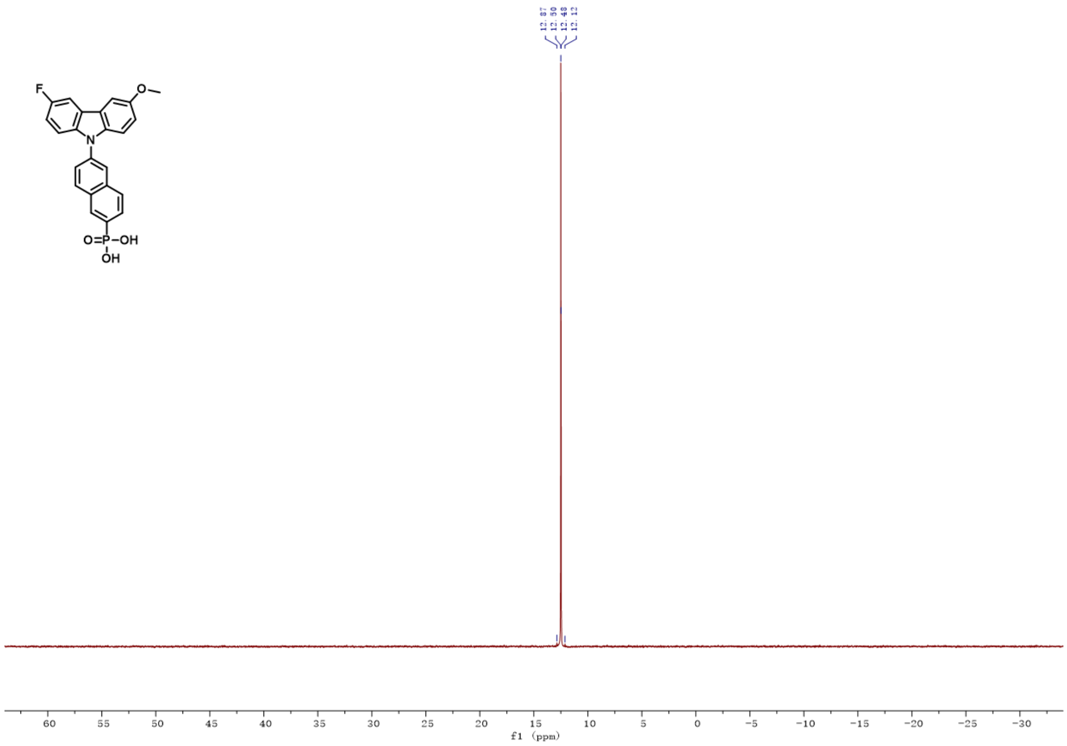

Figure S6. ^{31}P NMR spectrum of MeOF-NaPACz in DMSO-d$_6$.

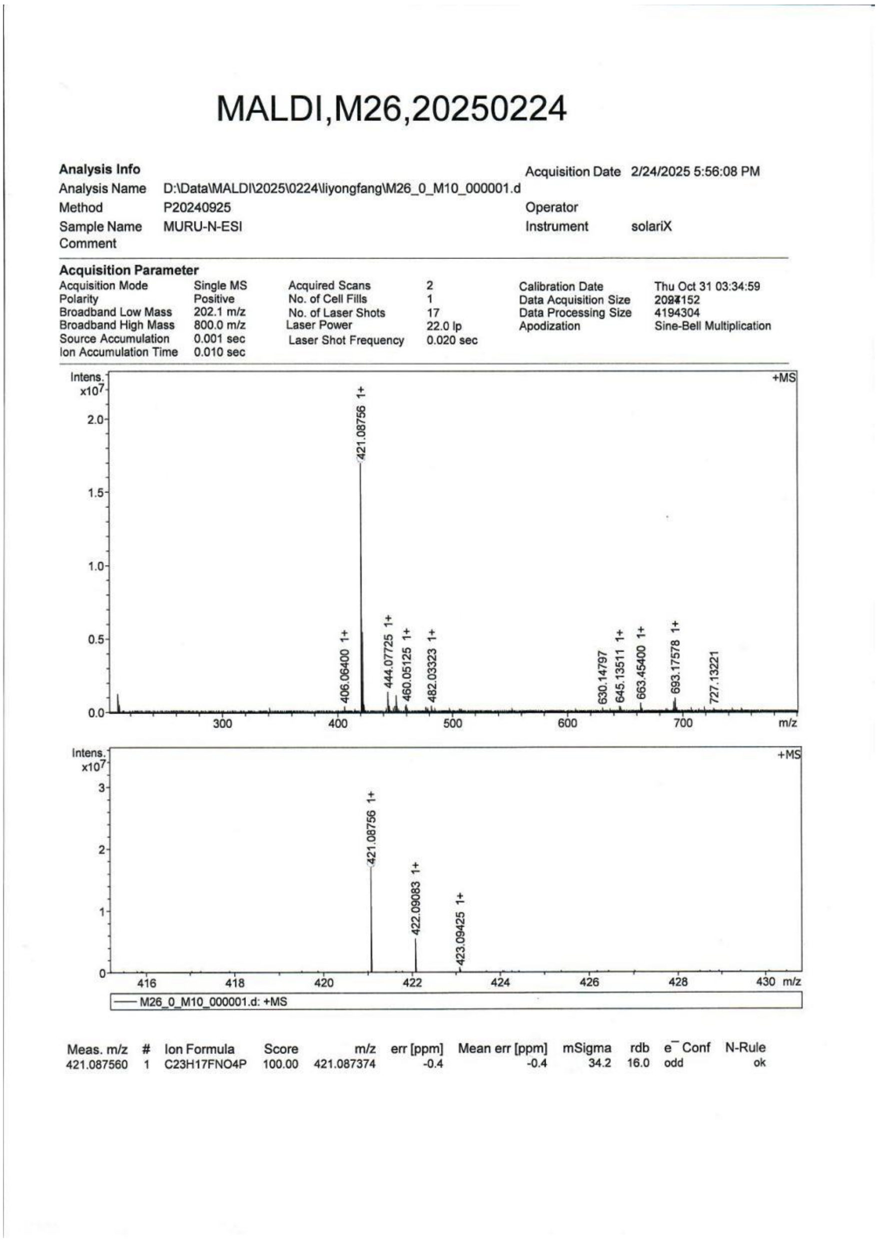

MALDI,M26,20250224

Analysis Info

Analysis Name D:\Data\MALDI\2025\0224\liyongfang\M26_0_M10_000001.d
Method P20240925
Sample Name MURU-N-ESI
Comment
Acquisition Date 2/24/2025 5:56:08 PM
Operator
Instrument solariX

Acquisition Parameter

Acquisition Mode	Single MS	Acquired Scans	2	Calibration Date	Thu Oct 31 03:34:59
Polarity	Positive	No. of Cell Fills	1	Data Acquisition Size	2097152
Broadband Low Mass	202.1 m/z	No. of Laser Shots	17	Data Processing Size	4194304
Broadband High Mass	800.0 m/z	Laser Power	22.0 lp	Apodization	Sine-Bell Multiplication
Source Accumulation	0.001 sec	Laser Shot Frequency	0.020 sec		
Ion Accumulation Time	0.010 sec				

Meas. m/z	#	Ion Formula	Score	m/z	err [ppm]	Mean err [ppm]	mSigma	rdb	e¯ Conf	N-Rule
421.087560	1	C23H17FNO4P	100.00	421.087374	-0.4	-0.4	34.2	16.0	odd	ok

Figure S7. Mass spectra of MeOF-NaPACz.

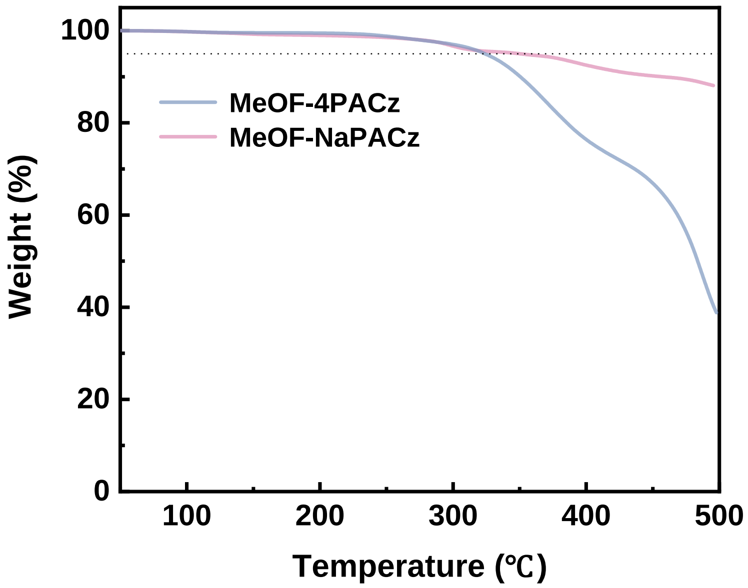

Figure S8. TGA curves of MeOF-4PACz and MeOF-NaPACz.

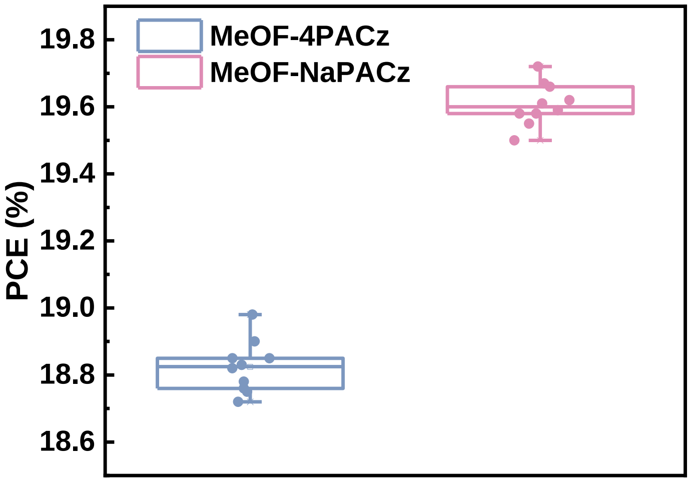

Figure S9. The distribution of device performance based on MeOF-4PACz and MeOF-NaPACz.

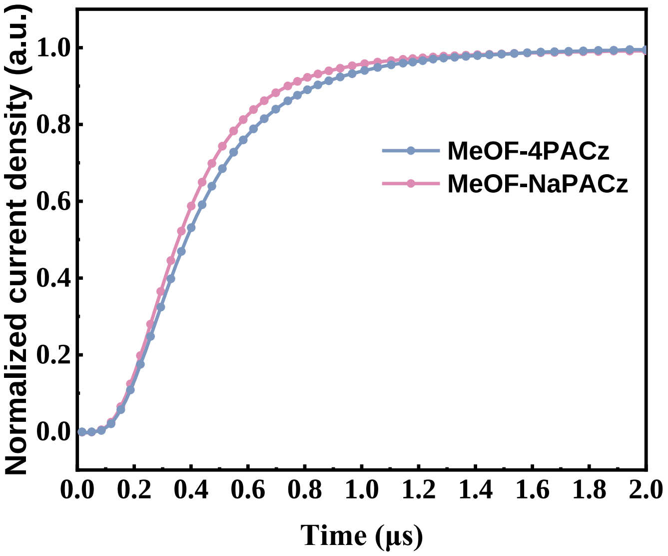

Figure S10. Charge extraction time of normalized TPC curves.

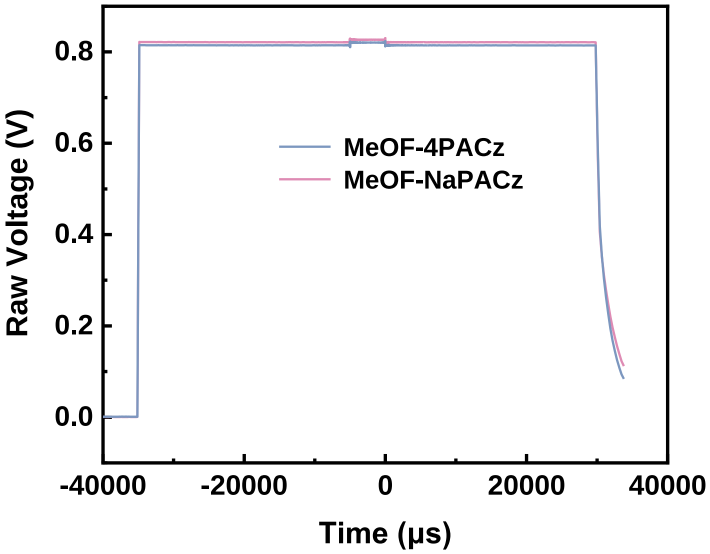

Figure S11. Original decay curves of TPV.

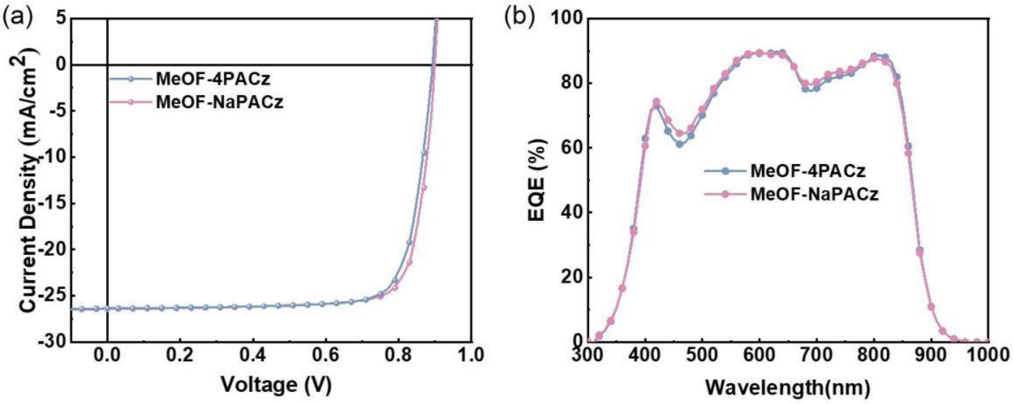

Figure S12. (a) *J-V* curves, (b) EQE curves of the optimized OSCs with PM6: L8-BO as the active layer and MeOF-4PACz or MeOF-NaPACz as the HTL under the illumination of AM 1.5G, 100 mW cm^{-2}.

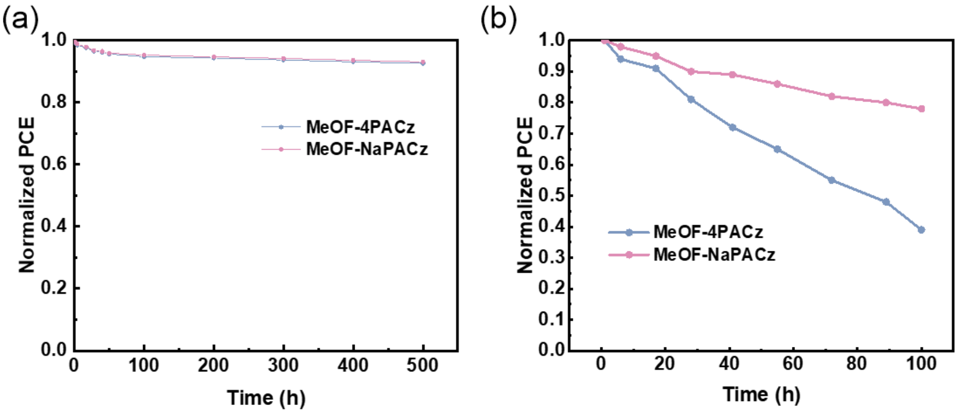

Figure S13. (a) Normalized PCE curves of devices with different SAMs under nitrogen atmosphere away from light. (b) Normalized PCE curves of devices with different SAMs under prolonged exposure to 85°C conditions.

Table S1. Calculated dipole moments of MeOF-4PACz, MeOF-NaPACz, Carbazole core, butylphosphonic acid and naphthalen-2-ylphosphonic acid.

	MeOF-4PACz	MeOF-NaPACz	Carbazole core	butylphosphonic acid	naphthalen-2- yl phosphonic acid
Dipole moment	2.27D	2.62D	1.98D	1.88D	2.58D

Table S2. The P:In intensity ratio of ITO substrates coated with different HTLs.

HTL on ITO	P $2p_{1/2}$ area	P $2p_{3/2}$area	P 2p area	In 3d3/2 area	P:In intensity ratio
MeOF-4PACz	494	992	1486	78069	0.019
MeOF-NaPACz	692	1355	2047	88726	0.023

Table S3. SAM atomic concentrations and calculations from XPS

HTL on ITO	C 1s area	P 2p area	$R_{\text{intensity}}$	R_{ASF}	R_{number}	$R_{\text{ASF}}/R_{\text{number}}$
MeOF-4PACz	11847	1486	7.97	12.43	17	0.73
MeOF-NaPACz	25571	2047	12.49	19.48	23	0.85

Reference

[1] Chen Z, Li X, Qin S, Gong Y, Liu Z, Yuan M, Liang T, Meng L, Li Y. *CCS Chemistry*, 2024, 7: 507-518